

Electronic Supporting Information

The Interplay of Chemical Bonding and Thermoelectric Properties in Doped Cubic GeTe

Sree Sourav Das,^a Safoura Nayeb Sadeghi,^b Keivan Esfarjani^{b,c,d} and Mona Zebarjadi^{*a,c}

Number of Bands for projections:

To determine the required number of wavefunctions for the projection from plane waves to atomic orbitals for COHP calculation, the DFT calculations must include enough bands in the self-consistent calculations. The number of bands depends on the structure and the basis used for the projection in LOBSTER. The calculation of the minimum number of bands for different supercells is discussed here.

For GeTe,

With the basis: Ge(4s²4p²3d¹⁰), Te(5s²5p⁴4d¹⁰).

There are 27 Ge atoms and 27 Te atoms in the supercell.

Minimum number of bands:

$$\frac{27[2(Ge - 4s) + 2(Ge - 4p) + 10(Ge - 3d) + 2(Te - 5s) + 4(Te - 5p) + 10(Te - 4d)]}{2} = 405$$

For Pb:GeTe, 2 Ge atoms is replaced by Pb atoms

With the basis: Pb(6s²6p²5d¹⁰)

Minimum number of bands:

$$\frac{25[2(Ge - 4s) + 2(Ge - 4p) + 10(Ge - 3d)] + 27[2(Te - 5s) + 4(Te - 5p) + 10(Te - 4d)] + 2}{2} = 405$$

For Bi:GeTe, 2 Ge atoms is replaced by Bi atoms

With the basis: Bi(6s²6p³5d¹⁰)

Minimum number of bands:

$$\frac{25[2(Ge - 4s) + 2(Ge - 4p) + 10(Ge - 3d)] + 27[2(Te - 5s) + 4(Te - 5p) + 10(Te - 4d)] + 2}{2} = 406$$

For Sb:GeTe, 2 Ge atoms is replaced by Sb atoms

With the basis: Sb(5s²5p³)

Minimum number of bands:

$$\frac{25[2(Ge - 4s) + 2(Ge - 4p) + 10(Ge - 3d)] + 27[2(Te - 5s) + 4(Te - 5p) + 10(Te - 4d)] + 2[2(Sb - 5s) + 3(Sb - 5p)]}{2} = 396$$

For In:GeTe, 2 Ge atoms is replaced by In atoms

With the basis: In(5s²5p¹4d¹⁰)

Minimum number of bands:

$$\frac{25[2(Ge - 4s) + 2(Ge - 4p) + 10(Ge - 3d)] + 27[2(Te - 5s) + 4(Te - 5p) + 10(Te - 4d)] + 2}{2} = 404$$

Summary of dopant elements in GeTe:

As-grown GeTe is predominantly a highly p-doped degenerate narrow gap semiconductor due to a high level of Ge vacancies. The introduction of additional dopants in GeTe is to lower the high hole concentration by effective suppression of intrinsic Ge vacancies and concurrently modifying the electronic structure. In recent years, significant efforts have been made to improve the performance of GeTe by introducing different dopants in it as shown in Fig. 1 in the main text. Fig. S1 summarizes the collective insights gleaned from the literature, showcasing the impactful advancements made in recent years.

1 H Hydrogen lightblue																	2 He Helium lightblue
3 Li Lithium lightblue	4 Be Beryllium lightblue											5 B Boron lightblue	6 C Carbon lightblue	7 N Nitrogen lightblue	8 O Oxygen lightblue	9 F Fluorine lightblue	10 Ne Neon lightblue
11 Na Sodium lightblue	12 Mg Magnesium orange											13 Al Aluminum orange	14 Si Silicon lightblue	15 P Phosphorus lightblue	16 S Sulfur lightblue	17 Cl Chlorine lightblue	18 Ar Argon lightblue
19 K Potassium lightblue	20 Ca Calcium lightblue	21 Sc Scandium orange	22 Ti Titanium orange	23 V Vanadium orange	24 Cr Chromium orange	25 Mn Manganese orange	26 Fe Iron lightblue	27 Co Cobalt lightblue	28 Ni Nickel lightblue	29 Cu Copper orange	30 Zn Zinc orange	31 Ga Gallium lightblue	32 Ge Germanium lightblue	33 As Arsenic lightblue	34 Se Selenium lightblue	35 Br Bromine lightblue	36 Kr Krypton lightblue
37 Rb Rubidium lightblue	38 Sr Strontium lightblue	39 Y Yttrium orange	40 Zr Zirconium orange	41 Nb Niobium lightblue	42 Mo Molybdenum lightblue	43 Tc Technetium lightblue	44 Ru Ruthenium lightblue	45 Rh Rhodium lightblue	46 Pd Palladium lightblue	47 Ag Silver orange	48 Cd Cadmium orange	49 In Indium orange	50 Sn Tin orange	51 Sb Antimony orange	52 Te Tellurium lightblue	53 I Iodine lightblue	54 Xe Xenon lightblue
55 Cs Cesium lightblue	56 Ba Barium lightblue	57 La Lanthanum lightblue	72 Hf Hafnium lightblue	73 Ta Tantalum lightblue	74 W Tungsten lightblue	75 Re Rhenium orange	76 Os Osmium lightblue	77 Ir Iridium lightblue	78 Pt Platinum lightblue	79 Au Gold lightblue	80 Hg Mercury lightblue	81 Tl Thallium lightblue	82 Pb Lead orange	83 Bi Bismuth orange	84 Po Polonium lightblue	85 At Astatine lightblue	86 Rn Radon lightblue
87 Fr Francium lightblue	88 Ra Radium lightblue	89 Ac Actinium lightblue	104 Rf Rutherfordium lightblue	105 Db Dubnium lightblue	106 Sg Seaborgium lightblue	107 Bh Bohrium lightblue	108 Hs Hassium lightblue	109 Mt Meitnerium lightblue	110 Ds Darmstadtium lightblue	111 Rg Roentgenium lightblue	112 Cn Copernicium lightblue	113 Nh Nihonium lightblue	114 Fl Flerovium lightblue	115 Mc Moscovium lightblue	116 Lv Livermorium lightblue	117 Ts Tennessine lightblue	118 Og Oganesson lightblue
		58 Ce Cerium lightblue	59 Pr Praseodymium lightblue	60 Nd Neodymium lightblue	61 Pm Promethium lightblue	62 Sm Samarium lightblue	63 Eu Europium lightblue	64 Gd Gadolinium lightblue	65 Tb Terbium lightblue	66 Dy Dysprosium lightblue	67 Ho Holmium lightblue	68 Er Erbium orange	69 Tm Thulium lightblue	70 Yb Ytterbium lightblue	71 Lu Lutetium orange		
		90 Th Thorium lightblue	91 Pa Protactinium lightblue	92 U Uranium lightblue	93 Np Neptunium lightblue	94 Pu Plutonium lightblue	95 Am Americium lightblue	96 Cm Curium lightblue	97 Bk Berkelium lightblue	98 Cf Californium lightblue	99 Es Einsteinium lightblue	100 Fm Fermium lightblue	101 Md Mendelevium lightblue	102 No Nobelium lightblue	103 Lr Lawrencium lightblue		

Fig. S1 Summary of recently used dopant materials (orange color) in GeTe achieving zT>1.0

Phonon Dispersion:

As cubic-GeTe is not thermodynamically stable at room temperature, vibrational modes are stabilized by a finite temperature of 800 K in TDEP calculations as depicted in Fig. 5(b) whereas density functional perturbation calculation reveals imaginary phonon modes as shown in Fig. S2.

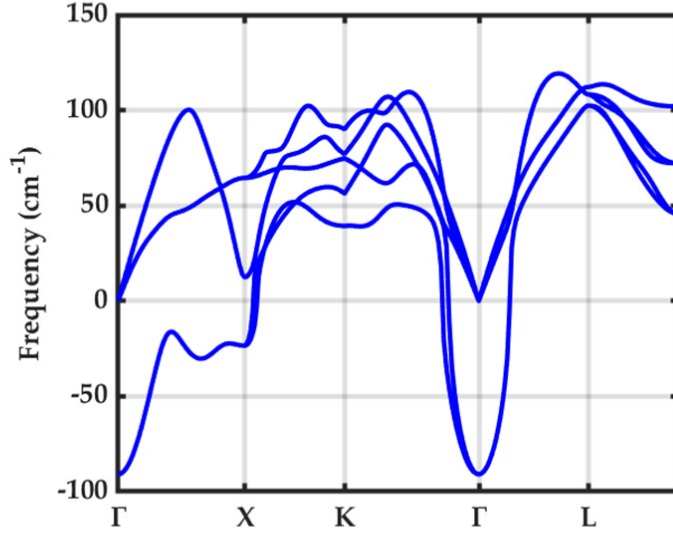


Fig. S2 Phonon dispersion computed from dynamical matrix using 4x4x4 q-point mesh.

Elastic constants from group velocities:

In a cubic crystal, using elasticity theory, it is possible to extract the 3 independent elastic constants from the acoustic group velocities along [110] direction. We have used the following relations to complete the table 2 in the main text:

$$\rho v_{t,z}^2 = C_{44}; \rho v_{t,xy}^2 = \frac{(C_{11} - C_{12})}{2}; \rho v_l^2 = \frac{(C_{11} + C_{12})}{2} - C_{44}$$

Where the mass density $\rho=6115.5 \text{ kg/m}^3$; and for $q=[110]$ the two transverse group velocities are polarized along z (for the shear mode C_{44}), and in the xy plane.

Convergence Study of K-mesh and q-mesh:

Before performing the transport calculations, convergence of electron-phonon scattering rates has been performed with varying k-mesh and q-mesh. Fig. S3(a-b) depicts the change in electron-phonon scattering rates with q-mesh and k-mesh. It is evident that k-mesh of $60 \times 60 \times 60$ and q-mesh 5×10^6 would be enough to reach convergence. This has been further validated by transport properties as shown in Fig. S3(c-d).

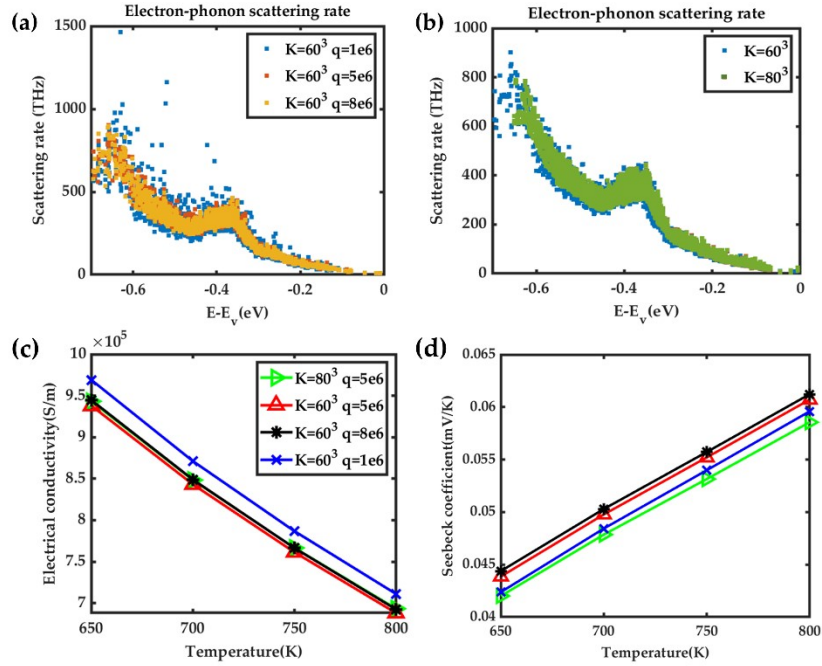


Fig. S3 Convergence study of K-mesh and q-mesh (a) q-mesh dependent electron-phonon scattering rates with fixed k-mesh $60 \times 60 \times 60$, (b) K-mesh dependent electron-phonon scattering rates with fixed q-mesh of 5×10^6 , (c) electrical conductivity, (d) Seebeck coefficient including only electron-phonon scattering with respect to different k-mesh and q-mesh.

Valence electron wavefunction:

As explained in the main text, the conduction band of cubic-GeTe is governed by Ge(p) orbital and the valence band is from Ge(s) and Te(p) orbitals. This is revealed by electron wavefunction plot in Fig. S4 where Fig. S4(a) & (b) shows the Ge(p)-Te(p) interactions and Ge(s)-Te(p) interactions, respectively.

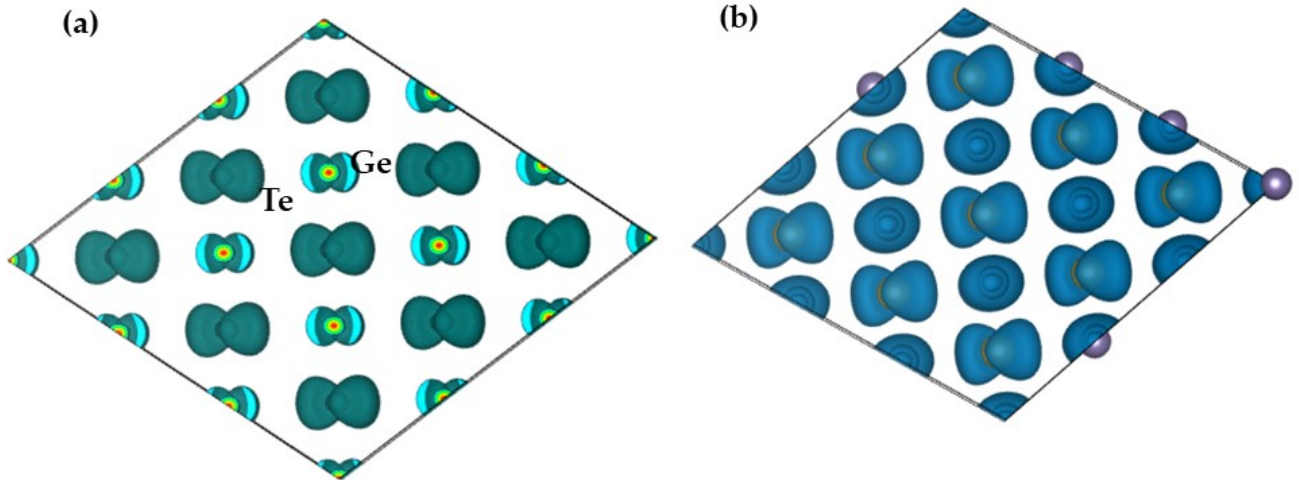


Fig. S4 Isosurfaces of the valence electron wavefunction at (a) 20% of the isovalue (Ge(p)-Te(p) interactions), (b) 10% of isovalue (Ge(s)-Te(p) interactions).

Projected Density of States:

Projected density of states (PDOS) for all supercells is shown in Fig. S5.

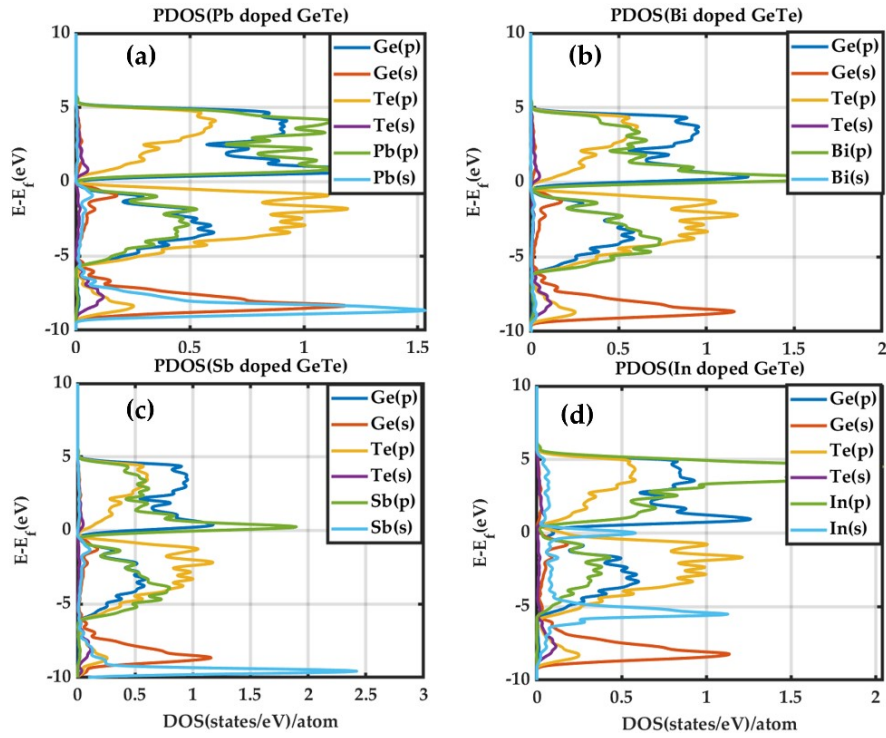


Fig. S5 Projected density of states (PDOS) (a) Pb doped GeTe, (b) Bi doped GeTe, (c) Sb doped GeTe, and (d) In doped GeTe.

The contribution of orbital projected PDOS to total DOS in Fig. S6 shows that s-contribution from dopants (X) in valance band decreases as $X=In, Pb, Sb, Bi$. Except Indium, other dopants do not have significant effect on total dos (Fig. S6(e)) rather than changing the fermi level.

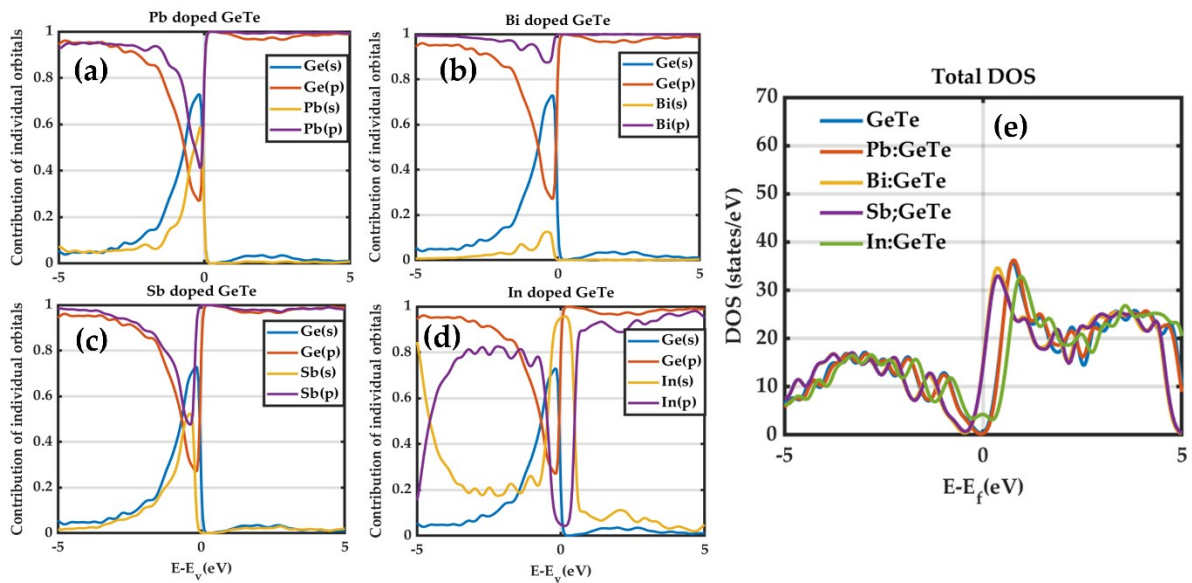


Fig. S6 Contribution of s and p orbital on DOS (a) Pb doped GeTe, (b) Bi doped GeTe, (c) Sb doped GeTe, (d) In doped GeTe, w.r.t valance band minimum and (e) total DOS w.r.t fermi level for all samples.

Table S1: ICOHP of s-p interactions in doped GeTe showing that the Te-X bonds become more antibonding (weaker) as X=In, Ge, Sb, Pb, Bi

Bonding	ICOHP for s-p (eV)
In-Te	-0.34
Ge-Te	-0.132
Sb-Te	-0.11
Pb-Te	-0.094
Bi-Te	-0.072

Electronic Band Structure comparison:

Fig. S7 (a) shows the electronic band structure with and without spin-orbit coupling (SOC). There is no significant effect of SOC on electronic band structure near the fermi level. Also wannierized band structure coincides well with DFT band structure.

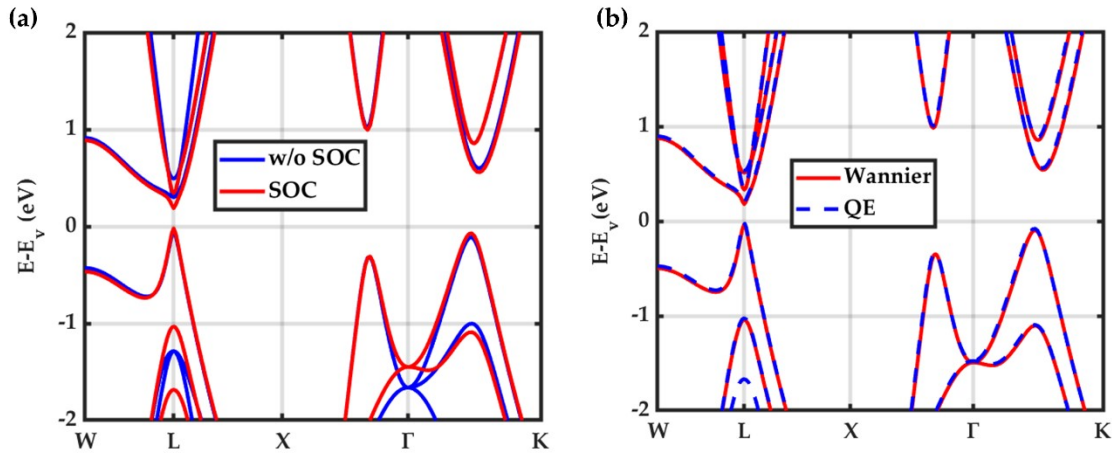


Fig. S7 (a) Electronic band structure with and without SOC, (b) Comparison between wannierized and DFT band structure.

Screening length:

Screening length is a strong function of carrier concentration compared to temperature as depicted in Fig. S8. At very high concentrations, electron-impurity screening length is shorter than low concentrations.

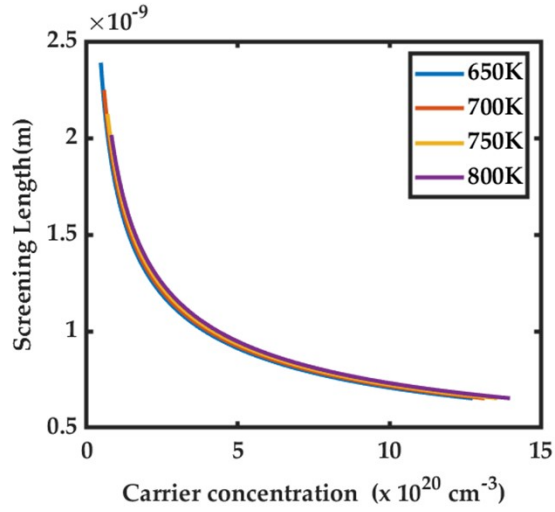


Fig. S8 Screening length versus carrier concentration at different temperatures.

Transport Properties of cubic-GeTe:

Semiclassical Boltzmann Transport formula under energy dependent relaxation time has been used for transport calculation.

Temperature and carrier concentration dependent transport coefficients are shown in Fig. S9.

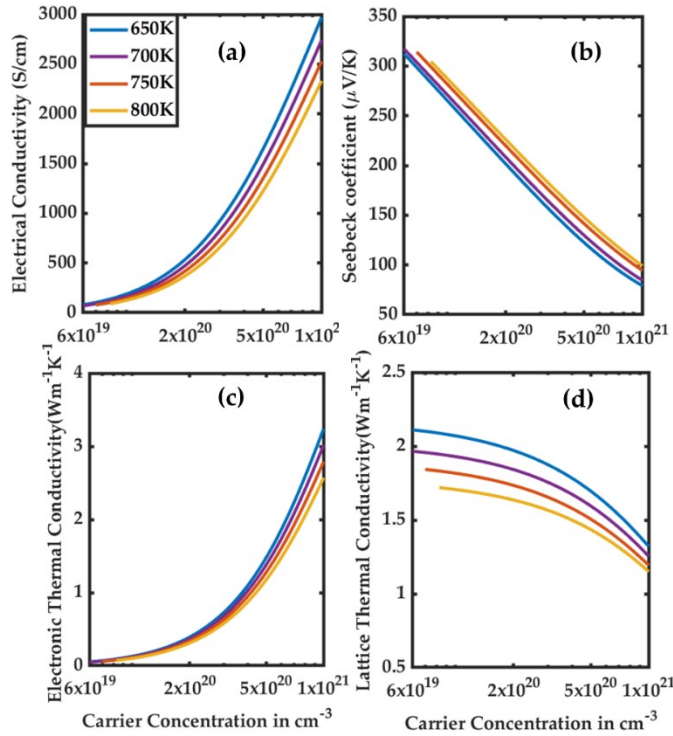


Fig. S9 Transport properties based on RTA (a) electrical conductivity, (b) Seebeck coefficient, (c) Electronic thermal conductivity, and (d) Lattice thermal conductivity.